Analysis of the Whole-Body Averaged Specific Absorption Rate (SAR) for Far-Field Exposure of an Isolated Human Body Using Cylindrical Antenna Theory

Behailu Kibret*, Assefa K. Teshome, and Daniel T. H. Lai

Abstract—This study proposes an accurate estimation of whole-body averaged specific absorption rate (WBA-SAR) for far-field exposure of an isolated human body in the frequency range of 10–200 MHz based on a lossy homogenous cylindrical antenna model of the human body. Equations are derived for the total induced axial current and the whole-body averaged SAR based on a rigorous treatment of cylindrical antenna theory. An explicit formula for the resonance frequency in terms of the anatomical parameters and the dielectric properties of the body is proposed for the first time. Moreover, important phenomena in far-field radio frequency (RF) dosimetry, such as, the cause of resonance and the SAR frequency characteristics are discussed from an antenna theory perspective.

1. INTRODUCTION

As the application of electromagnetic fields increases along with the progress of technology, there is also a growing concern in the society about its possible adverse effects. As a prevention from excessive heating due to electromagnetic exposure of the human body, the International Commission on Non-Ionizing Radiation Protection (ICNIRP) and the Institute of Electrical and Electronic Engineers (IEEE) have developed safety guidelines [1] and standards [2], respectively, that use the whole-body averaged specific absorption rate (WBA-SAR) as a proxy metric for temperature rise in the body. The ICNIRP guideline limits a WBA-SAR of $0.4\,\mathrm{Wkg}^{-1}$ for occupational exposure and $0.08\,\mathrm{Wkg}^{-1}$ for public exposure. Since it is inconvenient to measure SAR inside the human body, calculations are used to associate the SAR with measurable external electromagnetic field quantities, such as, the incident electric field; so that an exposure restriction can be imposed.

Early studies in electromagnetic dosimetry made use of simple geometrical shapes to model the human body so that analytical or simple numerical techniques could be applied [3, 4]. Utilising the progress in computational electromagnetics and computing power in the last two decades, several studies have investigated SAR based on anatomically realistic voxel models of the human body [5–7]. Also, complementing such studies, other studies have used the cylindrical antenna model of the human body to calculate the induced currents inside the human body when it is exposed to extremely low frequency (ELF), very low frequency (VLF) and radio frequency (RF) electromagnetic fields. King and Sandler [8] proposed an analytic method based on a two-term approximation of the current in a cylindrical antenna for the case of ELF and VLF exposure, in order to investigate electromagnetic field exposure from power transmission lines. Poljak and Roje [9] utilized the method of moments (MoM) to compute currents in a thick-wire model of human body in ELF exposure by employing the exact kernel of the Pocklington integro-differential equation. Both approaches provided reasonably accurate results compared to the results found using the finite-difference time-domain (FDTD) algorithm on voxel-based models of the

human body [10]. King extended his studies to 150 MHz [11] using similar analytic approaches; but the results were not as accurate as results reported by other authors. For example, the whole-body resonance frequency predicted by King for a grounded human body of height 1.75 m is near 53 MHz, which is different from the measured and calculated resonance frequency, near 40 MHz, reported by other authors [12]. One of the reasons for the deviation could be King's oversimplified assumption of using a single-term sinusoidal current in order to solve the two integral expressions inside the Hallén's type equation involved. Moreover, recently, the study of the human body antenna effect based on the cylindrical antenna model of the human body is reported by the authors of this paper [26]. In general, the ongoing acceptable trend of computing electromagnetic fields inside the human body makes use of the FDTD algorithm on realistic voxel-based models of the human body. In relation to this, though the analogy between the dipole antenna and the human body has been extensively reported, little has progressed in RF dosimetry analysis from an antenna theory perspective. This paper presents a simple but accurate technique to calculate the whole-body averaged SAR for far-field RF exposure based on the cylindrical antenna theory, which complements the results obtained through the FDTD.

It is known that the human body is anatomically more complicated than a homogenous cylinder. Therefore, unlike most of the previous papers, this paper does not attempt to approximate the human body with a cylinder; rather, it defines parameters of a cylindrical antenna based on the anatomical parameters of the human body so that the calculated WBA-SAR of the cylinder approximates that of the FDTD based WBA-SAR of the human body voxel models.

The results in this paper, from the representation of the human body as a cylindrical antenna, are validated by comparing them to the results from other authors who used the FDTD on the voxel models of two adult males (NORMAN and TARO), two adult females (NAOMI and HANAKO) and two children (NORMAN 10 Year and TARO 7 Year) that are described in [6, 7, 13, 14].

In this paper, firstly, the cylindrical antenna theory is applied to derive expressions for the total induced axial current and the WBA-SAR for a cylindrical antenna model of the human body. Then, the cylindrical antenna model is parameterised based on comparisons with the FDTD based results reported by other authors who used anatomically realistic voxel models. Furthermore, an explicit expression for the resonance frequency is derived. Finally, the effect of anatomy on the resonance frequency and the WBA-SAR is discussed.

2. WHOLE-BODY AVERAGED SAR FOR AN ISOLATED CYLINDER

The human body in standing position is represented by a homogenous cylindrical antenna that comprises muscle like tissue as shown in Figure 1. The dielectric property of muscle is calculated based on the 4-Cole-Cole dispersions that are parameterised by Gabriel et al. [15]. Therefore, the complex conductivity
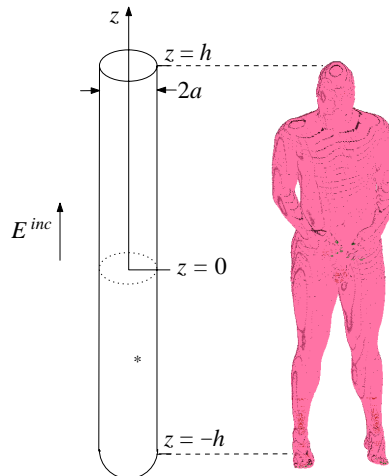
Figure 1. The cylindrical antenna model of the human body exposed to vertically polarised plane wave.

of muscle σ_{mus}^* as a function of the excitation angular frequency ω can be calculated as

$$\sigma_{mus}^* = j\omega\epsilon_0\epsilon_{mus}^* = \sigma_{eff} + j\omega\epsilon_0\epsilon \tag{1}$$

where ϵ_{mus}^* is the complex permittivity of muscle defined in [15], σ_{eff} the effective conductivity, and ϵ the relative permittivity. The permeability of the cylinder is taken to be equal to that of free space μ_0.

In this paper, it is assumed that a time-harmonic vertically polarized incident plane wave induces a rotationally symmetric current density in the cylinder of height $2h$ and radius a as shown in Figure 1. Working in a cylindrical coordinate system (ρ, ϕ, z) with the origin on the axis and at the midsection of the cylindrical antenna model, based on Taylor et al. [16], an approximate analytic expression for the total axial current can be derived as

$$I_{1z}(z) = \frac{j4\pi E^{inc}}{k_2\zeta_0}\left[H_U(\cos\gamma z - \cos\gamma h) + H_D\left(\cos\tfrac{1}{2}k_2 z - \cos\tfrac{1}{2}k_2 h\right)\right] \tag{2}$$

where $k_2 = \omega\sqrt{\epsilon_0\mu_0}$ is the free space wave number, $\zeta_0 = 120\pi\Omega$ the free space impedance, and E^{inc} the incident electric field at the surface of the cylinder. The imperfectly conducting nature of the cylinder is characterized by the parameter $\gamma = \beta - j\alpha$,

$$\gamma^2 = k_2^2\left(1 - \frac{j4\pi z^i}{k_2\zeta_0\Psi_{dR}}\right) \tag{3}$$

where z^i is impedance per unit length of the cylinder. According to King [17], z^i can be calculated as

$$z^i = \frac{\kappa}{2\pi a\sigma_\omega^*}\frac{J_0(\kappa a)}{J_1(\kappa a)} \tag{4}$$

where J_0 and J_1 are zeroth and first-order Bessel function, $\kappa^2 = k_1^2 - \gamma^2$. σ_ω^* is the complex conductivity of the cylinder, and $k_1 = \sqrt{j\omega\mu_0\sigma_\omega^*}$. The coefficients in (2) involve integrals that are computed numerically,

$$H_U = \frac{C_D - E_D}{C_U E_D - C_D E_U} \quad H_D = \frac{E_U - C_U}{C_U E_D - C_D E_U} \tag{5}$$

where

$$C_U = \left(1 - \frac{\gamma^2}{k_2^2}\right)(\Psi_{dUR} - \Psi_{dR})(1 - \cos\gamma h) - \frac{\gamma^2}{k_2^2}\Psi_{dUR}\cos\gamma h + j\Psi_{dUI}\left(\tfrac{3}{4} - \cos\tfrac{1}{2}k_2 h\right) + \Psi_U(h) \tag{6a}$$

$$C_D = \Psi_{dD}\left(\tfrac{3}{4} - \cos\tfrac{1}{2}k_2 h\right) - \left(1 - \frac{\gamma^2}{k_2^2}\right)\Psi_{dR}\left(1 - \cos\tfrac{1}{2}k_2 h\right) + \Psi_D(h) \tag{6b}$$

$$E_U = -\frac{\gamma^2}{k_2^2}\Psi_{dUR}\cos\gamma h - j\tfrac{1}{4}\Psi_{dUI}\cos\tfrac{1}{2}k_2 h + \Psi_U(h) \tag{6c}$$

$$E_D = -\tfrac{1}{4}\Psi_{dD}\cos\tfrac{1}{2}k_2 h + \Psi_D(h) \tag{6d}$$

$$\Psi_U(h) = \int_{-h}^{h}\left(\cos\gamma z' - \cos\gamma h\right)\frac{e^{-jk_2 R_h}}{R_h}dz' \tag{7a}$$

$$\Psi_D(h) = \int_{-h}^{h}\left(\cos\tfrac{1}{2}k_2 z' - \cos\tfrac{1}{2}k_2 h\right)\frac{e^{-jk_2 R_h}}{R_h}dz' \tag{7b}$$

$$\Psi_{dR} = \Psi_{dR}(z_m), \quad \begin{cases} z_m = 0, & k_2 h \le \pi/2 \\ z_m = h - \lambda/4, & k_2 h > \pi/2 \end{cases} \tag{8a}$$

$$\Psi_{dR}(z) = \csc\gamma(h - |z|)\int_{-h}^{h}\sin\gamma\left(h - |z'|\right)\left[\frac{\cos k_2 R}{R} - \frac{\cos k_2 R_h}{R_h}\right]dz' \tag{8b}$$

$$\Psi_{dUR} = [1 - \cos \gamma h]^{-1} \int_{-h}^{h} \left[\cos \gamma z' - \cos \gamma h \right] \left[\frac{\cos k_2 R_0}{R_0} - \frac{\cos k_2 R_h}{R_h} \right] dz' \tag{8c}$$

$$\Psi_{dD} = \left[1 - \cos \tfrac{1}{2} k_2 h \right]^{-1} \int_{-h}^{h} \left[\cos \tfrac{1}{2} k_2 z' - \cos \tfrac{1}{2} k_2 h \right] \left[\frac{e^{-jk_2 R_0}}{R_0} - \frac{e^{-jk_2 R_h}}{R_h} \right] dz' \tag{8d}$$

$$\Psi_{dUI} = - \left[1 - \cos \tfrac{1}{2} k_2 h \right]^{-1} \int_{-h}^{h} \left[\cos \gamma z' - \cos \gamma h \right] \left[\frac{\sin k_2 R_0}{R_0} - \frac{\sin k_2 R_h}{R_h} \right] dz' \tag{8e}$$

$$R = \left[(z - z')^2 + a^2 \right]^{\frac{1}{2}} \quad R_0 = \left[z'^2 + a^2 \right]^{\frac{1}{2}} \tag{8f}$$

$$R_h = \left[(h - z')^2 + a^2 \right]^{\frac{1}{2}} \tag{8g}$$

The value of γ is calculated by the process of iteration that is initialised by $\gamma = k_2$ to calculate z^i and Ψ_{dR}, which are in turn used to calculate γ. The iteration is found to be highly convergent; thus, the results after several iteration steps suffice to provide accurate approximation.

The time average power per unit length dissipated in the cylinder cross-section at z is

$$P_{av}(z) = \frac{1}{2} \mathrm{Re} \left(z^i \right) |I_{1z}(z)|^2. \tag{9}$$

Therefore, the whole-body averaged SAR of the cylinder (WBASAR$_{cyl}$) can be calculated as

$$\mathrm{WBASAR}_{cyl} = \frac{\int_{-h}^{h} P_{av}(z) dz}{W_{cyl}} = \frac{1}{2} \frac{\mathrm{Re}(z^i)}{W_{cyl}} \int_{-h}^{h} |I_{1z}(z)|^2 dz \tag{10}$$

where W_{cyl} [kg] is the weight of the cylinder, and it is related to the physical parameters of the human subject that is represented by the cylindrical antenna model. Since the current is directly proportional to the incident electric field in (2), for a given WBA-SAR, the root-mean-squared (r.m.s.) incident electric field E^{inc} can be calculated as

$$E^{inc} = \left[\frac{(\mathrm{WBASAR}) W_{cyl}}{\mathrm{Re}(z^i) \int_{-h}^{h} |I_{1z}^e(z)|^2 dz} \right]^{\frac{1}{2}} \tag{11}$$

where WBASAR [Wkg^{-1}] is the whole-body averaged SAR given, and the $I_{1z}^e(z)$ [A/Vm^{-1}] is the total induced axial current per unit incident electric field field, defined as

$$I_{1z}^e(z) = \frac{j4\pi}{k_2 \zeta_0} \left[H_U (\cos \gamma z - \cos \gamma h) + H_D \left(\cos \tfrac{1}{2} k_2 z - \cos \tfrac{1}{2} k_2 h \right) \right]. \tag{12}$$

3. PARAMETERS OF THE CYLINDRICAL ANTENNA MODEL

The radius of the cylinder is calculated by comparing the body-mass-index (BMI $= W/H^2$) of the human subject with that of a homogenous cylinder [18] comprising muscle like tissue as

$$a \propto \sqrt{\frac{W}{\pi \rho_m H}} \tag{13}$$

where ρ_m [kgm^{-3}] is the average density of the human body, W [kg] the weight of the human subject, and H [m] the height of the human subject. The dielectric property of the cylinder is characterized

by assuming it consists of a suspension of spherical particles (cells) with complex conductivity σ_s^* in a medium of complex conductivity σ_m^*; furthermore, it is assumed that $\sigma_s^* \ll \sigma_m^*$. Based on the Maxwell-Wagner effective medium theory [19], the effective complex conductivity of the cylinder σ_ω^* can be related by

$$\frac{\sigma_\omega^* - \sigma_m^*}{\sigma_\omega^* + 2\sigma_m^*} = (1-x)\frac{\sigma_s^* - \sigma_m^*}{\sigma_s^* + 2\sigma_m^*} \tag{14}$$

that can be simplified as

$$\sigma_\omega^* = \frac{2x}{3-x}\sigma_m^* \tag{15}$$

where x is the volume fraction of the medium. It is assumed that the volume of the medium is equivalent to that of the total body water inside the human body, which is associated with the lean-body-mass, LBM, or fat free mass of the body. Therefore, assuming a unity density, the volume fraction of the medium is approximated as

$$x \simeq \frac{LBM}{W} \tag{16}$$

where the lean-body-mass for males is computed as [20]

$$LBM = 0.3210W + 33.92H - 29.5336 \tag{17}$$

and for females

$$LBM = 0.29569W + 41.813H - 43.2933. \tag{18}$$

Generally, the fraction of total body water is between 0.71–0.74 for human subjects of normal BMI. When the complex conductivity of the medium is equal to that of muscle ($\sigma_m^* = \sigma_{mus}^*$), the complex conductivity of the cylinder becomes $\sigma_\omega^* \approx \frac{2}{3}\sigma_{mus}^*$, which is the same value used extensively for the dielectric property of a homogenous human body model [21]. This paper points to the possible explanation of the basis of using the 2/3 constant of proportionality.

4. RESULTS

It has been widely reported that WBA-SAR depends on the height, the dielectric properties of the body, the anatomy and the shape of the body. Therefore, in order for the cylindrical antenna model to predict the WBA-SAR value obtained from the FDTD analysis of voxel-based models of actual human bodies, the parameters of the cylinder (H, σ_ω^*, a and W_{cyl}) should be defined based on the parameters of the voxel models. So that, from the comparison of the six voxel models, best accuracy can be obtained if the following parametrisation is performed on the cylinder models.

The calculated WBA-SAR is in excellent agreement with the FDTD results if the constant of proportionality in the expression of the radius (13) is equal to $\sqrt{5}$. Moreover, as the human anatomy depends on sex, the dielectric property is defined with additional sex dependent factor, such that,

$$\sigma_\omega^* \simeq \frac{\%mus}{2}\frac{2x}{3-x}\sigma_{mus}^* \tag{19}$$

where $\%mus$ is fraction of muscle by mass, and it can be approximated as 0.43 for the male models and 0.33 for the females [23]. Similarly, the weight of the cylinder is also sex dependent; for the adult male models,

$$W_{cyl} = \frac{W}{x} = \frac{W^2}{0.321W + 33.92H - 29.5336} \tag{20}$$

for the adult females,

$$W_{cyl} = 1.12\frac{W}{x} = \frac{1.12W^2}{0.29569W + 41.813H - 43.2933} \tag{21}$$

and for the children,

$$W_{cyl} = 1.4\frac{W}{x} = \frac{1.4W^2}{0.321W + 33.92H - 29.5336}. \tag{22}$$

Applying the previous parametrisation on the cylindrical antenna models, the maximum induced total axial current $|I_{1z}(z)|$ occurs when

$$k_2 \left(1 - \left| \frac{j4\pi z^i}{k_2 \zeta_0 \Psi_{dR}} \right| \right)^{\frac{1}{2}} h \simeq \frac{\pi}{8}. \tag{23}$$

Equation (23) can be written in a quadratic form by replacing z^i with the expression in (4) as

$$k_2^2 - \left| \frac{j2}{\zeta_0 \Psi_{dR}} \frac{\kappa}{\sigma_\omega^*} \frac{J_0(\kappa a)}{J_1(\kappa a)} \right| \frac{k_2}{a} - \frac{1}{16} \left(\frac{\pi}{H} \right)^2 = 0 \tag{24}$$

where $H = 2h$ is the height of the cylinder. The term in the absolute value in (24) tends to remain constant irrespective of the complex conductivity and radii that are used as parameters for the six cylindrical antenna models; therefore, approximating it with a constant T and using $k_2 = \omega\sqrt{\epsilon_0 \mu_0} = \omega/c = 2\pi f_{res}/c$, the quadratic equation can be solved for the resonant frequency f_{res} as

$$f_{res} \simeq \frac{c}{4\pi} \left[\frac{T}{a} + \sqrt{\left(\frac{T}{a} \right)^2 + \frac{1}{4} \left(\frac{\pi}{H} \right)^2} \right] \tag{25}$$

where c is the speed of light in free space. The expression in (25) has a form similar to the resonance frequency expression of the resonant cylindrical dielectric cavity antenna [24]; and it implies that the resonance frequency depends on the height H, the dielectric property of the body T and the anatomy a. When the parameters of the six cylindrical antenna models are applied, T gets very close to 0.31. Therefore, the expression for the resonance frequency can be rewritten as

$$f_{res} \simeq \frac{c}{4\pi} \left[4.4923 \sqrt{\frac{\pi H}{W}} + \sqrt{20.181 \frac{\pi H}{W} + 0.25 \left(\frac{\pi}{H} \right)^2} \right] \tag{26}$$

where ρ_m in (13) is approximated as $1050\,\mathrm{kg\,m^{-3}}$. The comparison of the resonance frequencies calculated from (26) to the FDTD based resonance frequencies calculated for the six voxel models is shown in Table 1. It is to be noted that the value of T is different for little children and adults with large BMI. Particularly, the expression in (26) is very accurate for the normal BMI range, for which, the muscle percentage can be approximated by 43% for the males and 33% for the females.

Table 1. Calculated resonance frequencies.

Voxel Model	Height H (m)	Weight (kg)	f_{res} (MHz)	f_{res} (MHz) FDTD voxel	% error	H/λ_{res}
NORMAN	1.76	73	65.85	65	1.31	0.3866
NAOMI	1.63	60	70.15	70	0.21	0.3814
TARO	1.73	65	68.88	70	1.6	0.3974
HANAKO	1.60	53	73.47	74	0.72	0.3921
NORMAN 10 Year	1.38	33	86.24	85	1.46	0.3969
TARO 7 Year	1.20	23	96.85	95	1.95	0.3876

In the literature, it has been largely reported that the height to wavelength ratio (H/λ_{res}) at the resonance frequency approaches 0.4 [4, 6, 7, 21]; but, an adequate rationale has not been reported that sheds light on the phenomenon. Since the accurate formulation of the resonance frequency (26) proposed in this paper is a function of anatomical parameters and the dielectric properties of the body, it points to the possible explanation of the phenomenon observed.

The whole-body averaged SAR calculated using (10) is compared to the FDTD based results reported in [6, 13, 22] as shown in Figure 2. Moreover, the calculated incident electric field (11) required
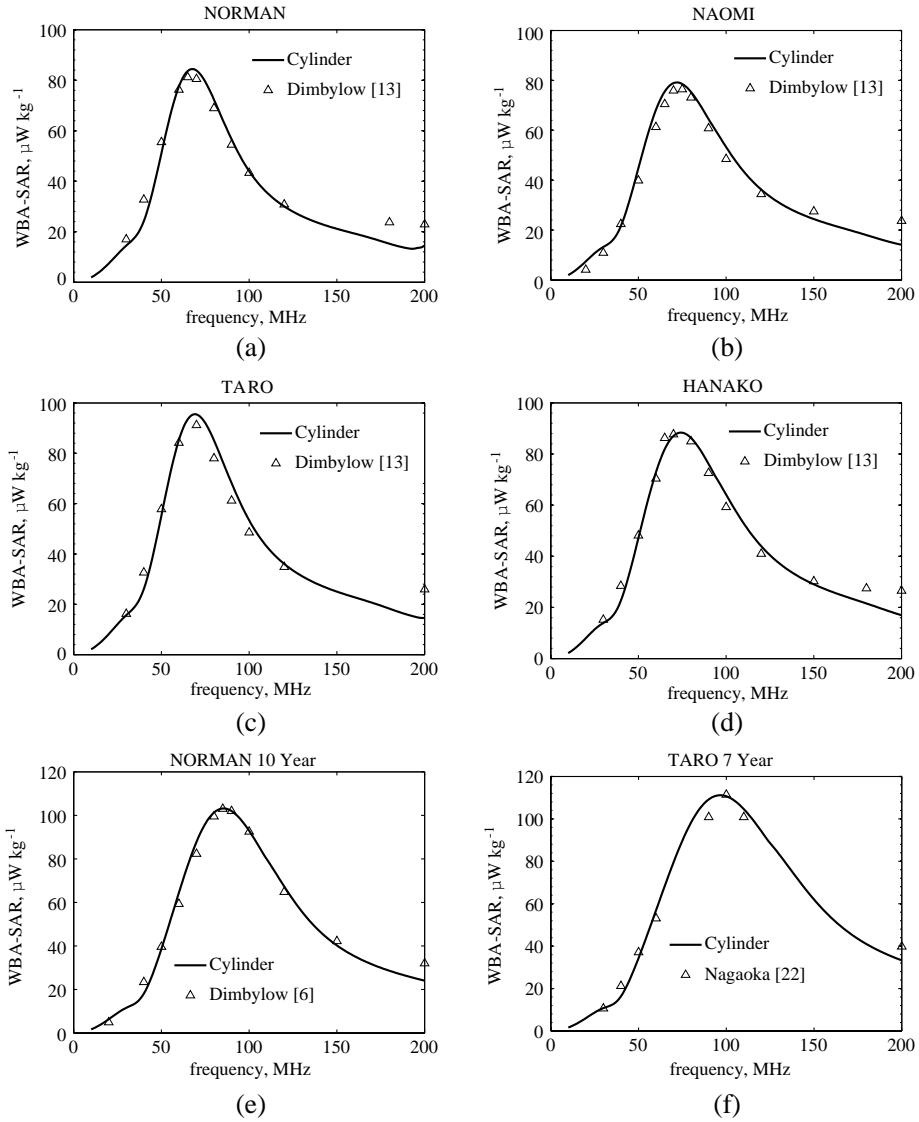
Figure 2. WBA-SAR from the cylindrical model (solid line) and the FDTD computed on voxel models by other authors (triangle markers) for an incident field $E^{inc} = \sqrt{2}\,\mathrm{Vm}^{-1}$ ($1\,\mathrm{Vm}^{-1}$ r.m.s.).
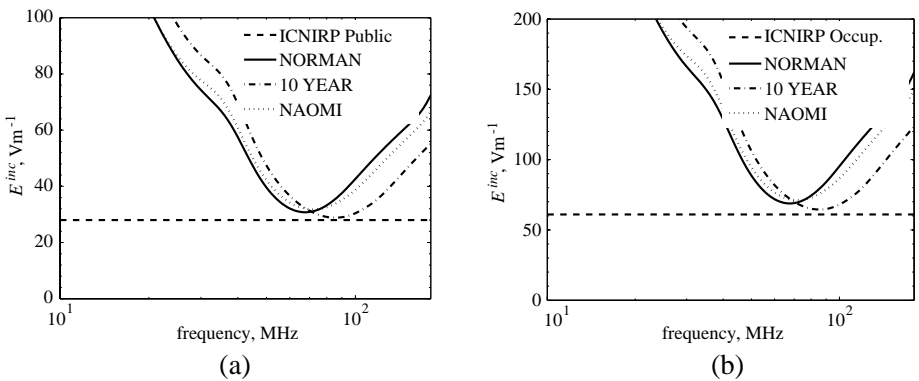
Figure 3. Calculated electric field values (r.m.s.) required to produce (a) the ICNIRP public and (b) occupational exposure restrictions on the WBA-SAR.

to produce the International Commission on Non-Ionising Radiation Protection (ICNIRP) occupational $(0.4\,\mathrm{Wkg}^{-1})$ and public $(0.08\,\mathrm{Wkg}^{-1})$ WBA-SAR restrictions are shown in Figure 3. From Figure 3, it can be seen that the incident electric field calculated for the 10 year old child model is too close to the ICNIRP reference level $(28\,\mathrm{Vm}^{-1}$ for public exposure and $61\,\mathrm{Vm}^{-1}$ for occupational exposure) [1], indicating that the proposed reference level may not provide a conservative estimate of WBA-SAR in children as reported by other studies [6].

5. DISCUSSION

The expression for the total induced axial current in (2) is derived based on the thin-wire approximation that puts the condition $k_2 a \ll 1$ and $h \gg a$, which is loosely satisfied by the frequency range 10–200 MHz. This implies that the calculated axial current for higher frequencies becomes less accurate; as a result, the calculated WBA-SAR starts to diverge from the FDTD results for frequencies higher than 150 MHz as shown in Figure 2. In short, the technique discussed here is more appropriate for the whole-body resonance frequency range. For the adult models, the WBA-SAR tends to remain constant for the frequencies higher than 200 MHz up to 3 GHz [13]; therefore, the frequency range considered in this study is relevant, as the WBA-SAR for the higher frequencies can be roughly approximated by the WBA-SAR value close to 200 MHz. In addition to this, it should be noted that the equation for the total axial current (2) is valid for vertically polarized incident electric field.

The expression for the total induced axial current (2) involves integrals that are computed numerically. When the computation is carried out using Matlab running on an ordinary PC, the computation time required to compute the WBA-SAR for 10–200 MHz is less than 10 seconds. This is a large time improvement over FDTD computations for voxel models that require extensive computing power. In addition, our approach is comparable in accuracy.

From the explicit expression of the resonance frequency in (25), interesting connections of the resonance frequency and a person's anatomy can be predicted. For example, assuming the adult male model, NORMAN, gained 7 kg of weight and also assuming the weight gain is not due to an increase in muscle mass, the value of the constant T in (25) changes slightly from 0.31 to 0.32. This causes the resonance frequency to shift from 65.8 MHz to 64.9 MHz. On the other hand, if NORMAN is 6 cm shorter with the same weight and $T = 0.32$, the resonance frequency shifts to 66.8 MHz. This implies that the resonance frequency for a person with high percentage fat is slightly smaller compared to that of a slender person of the same height. It also implies that a tall person has lower resonance frequencies compared to that of a shorter person of equivalent weight assuming that both have equal muscle mass. Overall, the effect of height is more pronounced than that of weight. These predictions are summarized in Table 2. In relation to this, the weight increase in NORMAN caused the WBA-SAR to decrease by approximately $6.5\,\mathrm{\mu Wkg}^{-1}$ for the frequencies higher than the resonance frequency and with insignificant change for the frequencies lower than the resonance frequency. This implies that the weight gain due to body fat might decrease the WBA-SAR for frequencies higher than the resonance frequency. But, the height difference in NORMAN modestly and uniformly decreased the WBA-SAR by approximately $1.47\,\mathrm{\mu Wkg}^{-1}$.

From antenna theory, it is known that a lossy and thick cylindrical antenna has a broadband frequency response [25]. A similar effect is also exhibited in the frequency characteristics of the WBA-SAR. If the cylindrical antenna model representing NORMAN is allowed to have a complex conductivity equal to that of the muscle tissue $(\sigma_\omega^* = \sigma_{mus}^*)$, the calculated WBA-SAR has a narrower frequency characteristics compared with that of the FDTD based result, as shown in Figure 4. On the other hand,

Table 2. Relationship between the anatomy and the resonance frequency based on NORMAN.

Height H (m)	Weight (kg)	f_{res} (MHz)
1.76	73	65.85
1.76	80	64.9
1.70	73	66.8
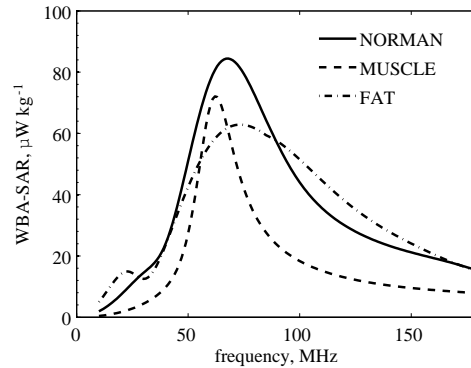
Figure 4. Comparison of different dielectric properties for the cylindrical model.

if the complex conductivity of the cylindrical antenna model is equal to that of fat tissue, the WBA-SAR has a broader frequency characteristics. This explains the narrower frequency characteristics of the adult male models compared to that of the females, as the females have lower muscle percentage by mass.

6. CONCLUSION

The cylindrical antenna theory is applied to formulate the total induced axial current and the WBA-SAR inside a cylindrical antenna model of the human body. The cylindrical antenna model is parameterised based on the anatomical parameters of six voxel models. From this, we propose a mathematical model for the resonance frequency, which points to the possible explanation of the relation between the height and the resonance wavelength, $H/\lambda_{res} \approx 0.4$. Moreover, important characteristics of the WBA-SAR, such as, the effect of weight, height and dielectric properties of the body are discussed. In general, this paper complements the results obtained through FDTD on realistic voxel model of the human body, by interpreting the results from antenna theory perspective. Future work will investigate models of WBA-SAR with a grounded human body.

REFERENCES

1. ICNIRP (International Commission on Non-Ionising Radiation Protection), "Guidelines for limiting exposure to time-varying electric, magnetic, and electromagnetic fields (up to 300 GHz)," *Health Phys.*, Vol. 74, No. 4, 494–522, 1998.
2. IEEE (Institute of Electrical and Electronics Engineers), "IEEE standard for safety levels with respect to human exposure to radio frequency electromagnetic fields, 3 kHz to 300 GHz," *Health Phys.*, C95-1, 2005.
3. Durney, C. H., "Electromagnetic dosimetry for models of humans and animals: A review of theoretical and numerical techniques," *Proc. IEEE*, Vol. 68, 33–40, 1980.
4. Ghandi, O. P., "State of the knowledge for electromagnetic absorbed dose in man and animals," *Proc. IEEE*, Vol. 68, No. 1, 24–32, 1980.
5. Dimbylow, P. J., "FDTD calculations of the whole-body average SAR in an anatomically realistic voxel model of the human body from 1 MHz to 1 GHz," *Phys. Med. Biol.*, Vol. 42, No. 3, 479–490, 1997.
6. Dimbylow, P. J., "Fine resolution calculations of SAR in the human body for frequencies up to 3 GHz," *Phys. Med. Biol.*, Vol. 47, No. 16, 2835–2846, 2002.
7. Wang, J., O. Fujiwara, S. Kodera, and S. Watanabe, "FDTD calculation of whole-body average SAR in adult and child models for frequencies from 30 MHz to 3 GHz," *Phys. Med. Biol.*, Vol. 51, No. 17, 4119–4127, 2006.

8. King, R. W. P. and S. S. Sandler, "Electric fields and currents induced in organs of the human body when exposed to ELF and VLF electromagnetic fields," *Radio Science*, Vol. 31, No. 5, 1153–1167, 1996.

9. Poljak, D. and V. Roje, "Currents induced in human body exposed to the power line electromagnetic field," *Proc. 20th Annu. Conf. IEEE Eng. Med. Biol. Soc.*, Vol. 6, 3281–3284, 1998.

10. Ghandi, O. P. and J. Chen, "Numerical dosimetry at power-line frequencies using anatomically based models," *Bioelectromagnetics Suppl.*, Vol. 13, No. S1, 43–60, 1992.

11. King, R. W. P., "Electric current and electric field induced in the human body when exposed to an incident electric field near the resonant frequency," *IEEE Trans. Microwave Theory and Tech.*, Vol. 48, No. 9, 1537–1543, 2000.

12. Ghandi, O. P., J. Chen, and A. Riazi, "Currents induced in a human being for plane-wave exposure conditions 0–50 MHz and for RF sealers," *IEEE Trans. Biomed. Eng.*, Vol. 33, No. 8, 757–767, 1986.

13. Dimbylow, P. J., A. Hirata, and T. Nagaoka, "Intercomparison of whole-body averaged SAR in European and Japanese voxel phantoms," *Phys. Med. Biol.*, Vol. 53, No. 20, 5883–5897, 2008.

14. Nagaoka, T., S. Watanabe, K. Sakurai, E. Kunieda, S. Watanabe, M. Taki, and Y. Yamanaka, "Development of realistic high-resolution whole-body voxel models of Japanese adult males and females of average height and weight, and application of models to radio-frequency electromagnetic-field dosimetry," *Phys. Med. Biol.*, Vol. 49, No. 1, 1–15, 2004.

15. Gabriel, S., R. Lau, and C. Gabriel, "The dielectric properties of biological tissues: III. Parametric models for the dielectric spectrum of tissues," *Phys. Med. Biol.*, Vol. 41, No. 11, 2271–2293, 1996.

16. Taylor, C. D., W. H. Charles, and A. A. Eugene, "Resistive receiving and scattering antenna," *IEEE Trans. Antennas Propag.*, Vol. 15, No. 3, 371–376, 1967.

17. King, R. W. P. and S. Prasad, *Fundamental Electromagnetic Theory and Applications*, Prentice-Hall, Englewood Cliffs, USA, 1986.

18. Heymsfield, S. B., A. Martin-Nguyen, T. M. Fong, M. Tung, D. Gallagher, and A. Pietrobelli, "Body circumferences: Clinical implications emerging from a new geometric model," *Nutr. Metab.*, Vol. 5, 24, 2008.

19. Martinsen, O. G., S. Grimnes, and H. P. Schwan, "Interface phenomena and dielectric properties of biological tissue," *Encyclopedia of Surface and Colloid Science*, Vol. 20, 2643–2653, 2002.

20. Hume, R., "Prediction of lean body mass from height and weight," *J. Clin. Pathol.*, Vol. 19, No. 4, 389–391, 1966.

21. Hirata, A., O. Fujiwara, T. Nagaoka, and S. Watanabe, "Estimation of whole-body average SAR in human models due to plane-wave exposure at resonance frequency," *IEEE Trans. Electromagn. Compat.*, Vol. 52, No. 1, 41–48, 2010.

22. Nagaoka, T., E. Kunieda, and S. Watanabe, "Proportion-corrected scaled voxel models for Japanese children and their application to the numerical dosimetry of specific absorption rate for frequencies from 30 MHz to 3 GHz," *Phys. Med. Biol.*, Vol. 53, No. 23, 6695–6711, 2008.

23. El Habachi, A., E. Conil, A. Hadjem, E. Vazquez, F. M. Wong, A. Gati, G. Fleury, and J. Wiart, "Statistical analysis of whole-body absorption depending on anatomical human characteristics at a frequency of 2.1 GHz," *Nutr. Metab.*, Vol. 55, No. 7, 1875–1887, 2010.

24. Long, S. A., M. W. McAllister, and L. C. Shen, "The resonant cylindrical dielectric cavity antenna," *IEEE Trans. Antennas Propag.*, Vol. 31, No. 3, 406–412, 1983.

25. Balanis, C. A., *Antenna Theory: Analysis and Design*, John Wiley & Sons, New Jersey, USA, 2005.

26. Kibret, B., A. K. Teshome, and D. T. H. Lai, "Human body as antenna and its effect on human body communications," *Progress In Electromagnetics Research*, Vol. 148, 193–207, 2014.